



**RESEARCH ARTICLE**

# Exploration of highly selective fluorogenic 'on-off' chemosensor for $\text{H}_2\text{PO}_4^-$ ions: ICT-based sensing and ATPase activity profiling

Yogesh B. Wagh<sup>1</sup>  | Kundan C. Tayade<sup>2</sup> | Anil Kuwar<sup>1</sup> | Suban K. Sahoo<sup>3</sup> | Mayank<sup>4</sup> | Narinder Singh<sup>4</sup> | Dipak S. Dalal<sup>1</sup> 

<sup>1</sup>School of Chemical Sciences, Kavayitri Bahinabai Chaudhari North Maharashtra University, Jalgaon, (MS), India

<sup>2</sup>Department of Chemistry and Analytical Chemistry, Rajarshi Shahu Mahavidyalaya (Autonomous), Latur, India

<sup>3</sup>Department of Applied Chemistry, S. V National Institute Technology, 395007 Gujarat, Surat, India

<sup>4</sup>Department of Chemistry, Indian Institute of Technology, Ropar, Punjab, India

**Correspondence**

Dipak S. Dalal, School of Chemical Sciences, Kavayitri Bahinabai Chaudhari North Maharashtra University, Jalgaon - 425001 (MS), India.  
 Email: dsdalal2007@gmail.com

**Funding information**

Council of Scientific & Industrial Research (CSIR), New Delhi India, Grant/Award Number: CSIR-RA [Award No. 09/728(0036)/2019 (EMR-I)].

**Abstract**
**Abstract**

In this study, the recognition contour of Chemosensor **1** was investigated using semi-aqueous methanol ( $X_{\text{H}}$ , mole fraction = 0.31) for a range of anions and bioactive species. Host-receptor signalling based on the internal charge transfer mechanism for Chemosensor **1** was explored and reported. Structure of Chemosensor **1** and its plausible anion coordination based on hydrogen bonding is complemented with density functional theory. Consequently, we investigated the applicability of the synthesized probe in blood plasma, urine, tap water samples, and for monitoring of ATP in lysosomes by apyrase enzyme.

**KEYWORDS**

anion coordination, apyrase activity, ATPase activity, ICT-based chemosensor, quenching

## 1 | INTRODUCTION

Anions play important roles in environmental, chemical, and biological processes. Therefore, in recent years, the field of sensing anionic species has expanded and a myriad of chemosensors have been fabricated for target specific anions.<sup>[1-3]</sup> Among these various types of chemosensors, fluorogenic anion sensors have gained significant attention because of their superior selectivity and sensitivity, appreciable detection limit, real-time application, and lack of need for pre-treatment.<sup>[4,5]</sup> Detection of phosphate-based anionic species within environmental samples is critical for monitoring the health status of our ecosystems.<sup>[6]</sup> In this aspect, many reported host molecules have so far avoided using intramolecular and intermolecular hydrogen bonding for their anion binding in polar medium.<sup>[7-9]</sup> Over recent decades, many hydrogen bonding-based anion sensing chemosensors have been extensively investigated.

Phosphate ions are known for their critical role in signal transduction, energy storage, and many other biological processes.<sup>[10-12]</sup> The exact estimation of the concentration of phosphate ions within biological fluids therefore seems very crucial, and could provide useful information on Fanconi's syndrome, vitamin D deficiency, hyperparathyroidism, and many other diseases.<sup>[13]</sup> Moreover, dihydrogen phosphate anion ( $\text{H}_2\text{PO}_4^-$ ) is one of the main equilibrium species in biological and chemical systems containing inorganic phosphate. Therefore,  $\text{H}_2\text{PO}_4^-$  has become a research target for sensing.<sup>[14-16]</sup> Conversely, excess  $\text{H}_2\text{PO}_4^-$  in waterways, has been reported to be toxic.<sup>[17]</sup> Therefore, quantitative and qualitative determination of phosphate ions is of great importance in physiological studies.

The 2-iminothiazolidin-4-one core is a key heterocyclic class of organic compound, responsible for various type of biological activities.<sup>[18-20]</sup> As a part of our continued investigations into the

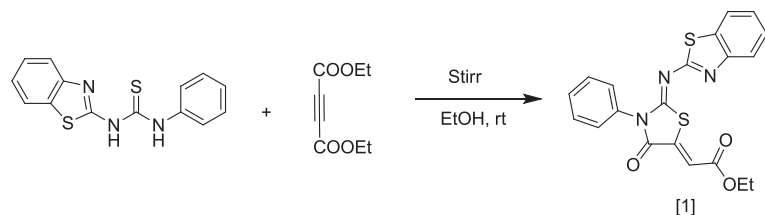
development of discern chemosensors,<sup>[21,22]</sup> we have previously reported a regioselective strategy for the synthesis of 2-imino-4-oxothiazolidin-5-ylidene acetates using substitution-dependent cyclization sequence, without any catalyst and at ambient temperature (Scheme 1).<sup>[23]</sup> Therefore we have extended its application in the synthesis of Chemosensor **1** and studied its ability to detect cations in semiaqueous medium.<sup>[24]</sup> Based on promising results from the previous study, Chemosensor (Z)-ethyl 2-((Z)-2-(benzo[d]thiazol-2-ylimino)-4-oxo-3-phenylthiazolidin-5-ylidene)acetate **1** was used here for sensing  $\text{H}_2\text{PO}_4^-$ , containing sulphur, nitrogen, and oxygen groups as recognition sites.

## 2 | EXPERIMENTAL

### 2.1 | Reagents and methods

All commercially available chemicals were procured from Sigma-Aldrich Ltd, India. To record UV-visible absorption and fluorescence spectra, a Shimadzu UV-3450 spectrophotometer and Fluoromax-4 spectrofluorometer were used, respectively. This included a scan range of 200–600 nm at room temperature (RT) and using a cuvette of 1 cm path length for this study. For the spectroscopic study, ultra-pure water and high performance liquid chromatography grade methanol was used to prepare solutions. Solutions of Chemosensor **1**, anions and biomolecules ( $c = 1$  mM and 0.01 mM) were prepared in  $\text{CH}_3\text{OH}/\text{H}_2\text{O}$  (50:50, v/v) followed by the preparation of requisite working solutions ( $c = 0.1$  mM). An anion selectivity study of Chemosensor **1** was performed fluorometrically for different anions ( $\text{F}^-$ ,  $\text{Cl}^-$ ,  $\text{Br}^-$ ,  $\text{I}^-$ ,  $\text{CH}_3\text{COO}^-$ ,  $\text{H}_2\text{PO}_4^-$ ,  $\text{NO}_3^-$ ,  $\text{CN}^-$ ,  $\text{HSO}_4^-$  and  $\text{HSO}_4^-$ ) as well as biomolecules (ATP, AMP, NADP, NADH, and NAD) at RT. To record the fluorescence intensity, wavelengths  $\lambda_{\text{ex}}/\lambda_{\text{em}} = 365/405$  nm were used alongside a reagent blank. The excitation and emission slits were set to 5.0 nm. The association constant ( $K_a$ ) and limit of detection were calculated from the titration experiments, which were performed between Chemosensor **1** and  $\text{H}_2\text{PO}_4^-$ . Titrations were performed using successive incremental additions of  $\text{H}_2\text{PO}_4^-$  ( $c = 0.1$  mM) to a fixed volume of Chemosensor **1** solution ( $c = 0.01$  mM) in a 10 ml volumetric flask.

The binding stoichiometry of the hydrogen-bonded anion coordination complex (Chemosensor **1**– $\text{H}_2\text{PO}_4^-$ ) was determined using Job's method. Here, the mole fraction was continuously varied, keeping the total concentration of Chemosensor **1** and  $\text{H}_2\text{PO}_4^-$  ions constant. These solutions are allowing to stand for 1 h with frequent shaking in-between. The fluorescence spectra were recorded for all mixtures.



The plot of  $[\text{HG}]$  versus  $X_{\text{H}}$  was used to determine the stoichiometry of the complex formed. Fluorescence intensity at 405 nm ( $\lambda_{\text{em}}$ ) was used for stoichiometry calculations. The concentration of  $[\text{HG}]$  was calculated using the equation  $[\text{HG}] = (\Delta F/F_0) [\text{H}]$  and  $X_{\text{H}} = \text{mole fraction} = [\text{H}]_{\text{v}}/([\text{H}]_{\text{v}} + [\text{G}]_{\text{v}})$ , where  $[\text{H}]$  represented the concentration of the free chemosensor.

## 3 | RESULTS AND DISCUSSION

Synthesis and characterization of Chemosensor **1**, along with the structural confirmation using single crystal X-ray diffraction were reported in our previous study.<sup>[24]</sup> The emission profile of Chemosensor **1** upon excitation at 365 nm revealed an emission band at 405 nm. The anion binding ability of Chemosensor **1** was investigated by adding various anions into its tetrabutylammonium salts form. The addition of all anions to Chemosensor **1** resulted in no change in the UV-visible spectrum. These results clearly revealed that Chemosensor **1** in its ground state did not bind with  $\text{H}_2\text{PO}_4^-$ .

When the fluorescence anion binding experiment was performed, most anions did not cause any significant changes, but following  $\text{H}_2\text{PO}_4^-$  addition instant quenching of the fluorescence emission band of Chemosensor **1** was observed (Figure 1). Upon addition of  $\text{H}_2\text{PO}_4^-$  to the Chemosensor **1** solution, instant quenching and a blue shift in its fluorescence emission band was observed. The fluorescence ratio metric response of Chemosensor **1** is displayed in Figure 2. From

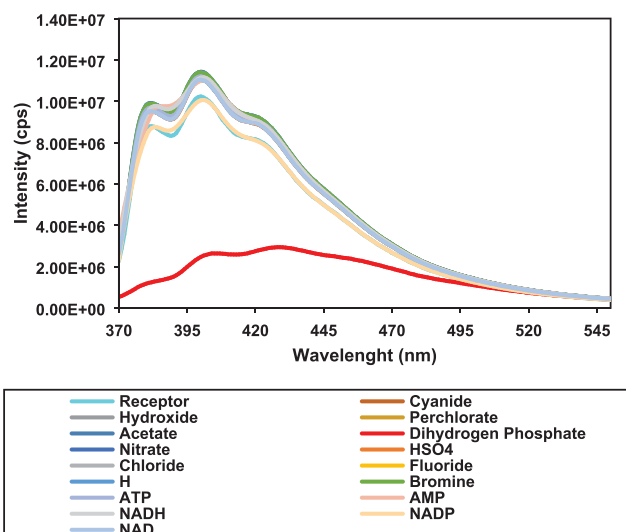


**FIGURE 1** Fluorescence profile of Chemosensor **1** (10  $\mu\text{M}$ ) upon addition of a particular anion/biomolecule (1 equiv.)

**SCHEME 1** Synthesis of Chemosensor **1**

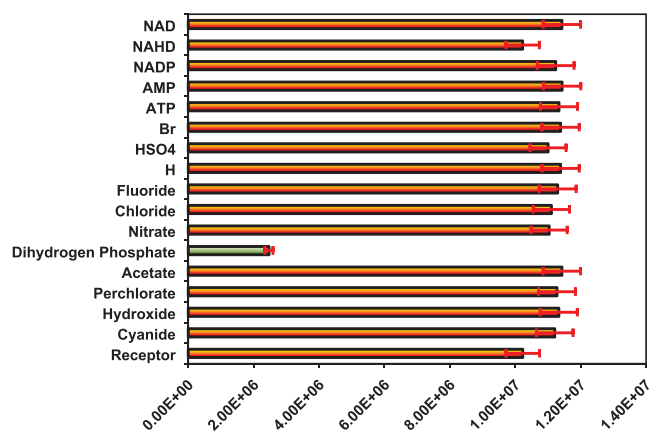


**FIGURE 2** Fluorescence ratiometric response of Chemosensor **1** ( $c = 1 \times 10^{-5}$  M) upon the addition of particular anions and biomolecules ( $c = 1 \times 10^{-4}$  M) in  $\text{CH}_3\text{OH}/\text{H}_2\text{O}$  (50:50, v/v)

Figure 2, it was confirmed that there was significant quenching in fluorescence intensity upon addition of  $\text{H}_2\text{PO}_4^-$ , and no prominent changes were observed with other entities. This quenching in fluorescence emission may result from the electron repelling effect of  $\text{H}_2\text{PO}_4^-$  and also partly result from the participation of the oxygen, sulphur, and imine-N for hydrogen bonding interaction with  $\text{H}_2\text{PO}_4^-$  which results in some structural or ring-size effects on the chemosensor in its the excited state.<sup>[25]</sup>

To further investigate the binding affinity of **1** as a chemosensor for  $\text{H}_2\text{PO}_4^-$ , fluorescence titration studies were performed. Upon incorporation of increasing concentrations of  $\text{H}_2\text{PO}_4^-$ , continuous quenching in the fluorescence behaviour of **1** was observed (Figure 3). Based on the titration results the detection limit, when estimated, was found to be as low as  $0.17 \mu\text{M}$   $\text{H}_2\text{PO}_4^-$  (Figure S1) which agrees with recently reported  $\text{H}_2\text{PO}_4^-$  sensors (Table S1), having a dynamic range of 0–15  $\mu\text{M}$  for  $\text{H}_2\text{PO}_4^-$ .

Job plot analysis<sup>[26]</sup> for binding between **1** and  $\text{H}_2\text{PO}_4^-$  revealed 1:1 stoichiometry (Figure S2) and the association constant

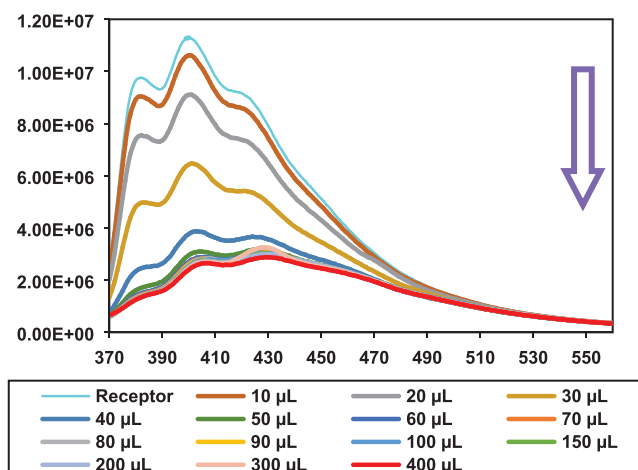


**FIGURE 3** Fluorescence titration of Chemosensor **1** ( $10 \mu\text{M}$ ) upon addition different concentrations of  $\text{H}_2\text{PO}_4^-$

calculated from the Benesi–Hildebrand plot was  $5.0 \times 10^6 \text{ M}^{-1}$  <sup>[27]</sup> (Figure S3).

Fluorescence quantum yield ( $\phi$ ) of Chemosensor **1** and its hydrogen-bonded anion coordination complex was evaluated. The quantum yield of Chemosensor **1** was found to be 0.161 and, upon Chemosensor **1**- $\text{H}_2\text{PO}_4^-$  complex formation, this was reduced to 0.147. Therefore, upon complex formation, the corresponding quantum yield also decreased significantly. This observation indicated that Chemosensor **1** was highly sensitive to  $\text{H}_2\text{PO}_4^-$  ions.

The practical applicability of Chemosensor **1** for  $\text{H}_2\text{PO}_4^-$  sensing was explored by performing competitive experiments with other probable interfering anions (one equivalent) in the presence of  $\text{H}_2\text{PO}_4^-$  ion at one equivalent of concentration. The resulting fluorescence curve for Chemosensor **1** plus one equivalent of  $\text{H}_2\text{PO}_4^-$  was not affected even in the presence of an excess of other interfering metal ions. (Figure 4). Based on these observations, it was concluded that Chemosensor **1** had good selectivity towards  $\text{H}_2\text{PO}_4^-$  over other competitive anions.

Optimization of structural features of the Chemosensor **1**- $\text{H}_2\text{PO}_4^-$  complex was performed using B3LYP in association with 6-311+G(d,p), and by considering the gaseous phase. Gaussian 09W software was used for all calculations.<sup>[28]</sup> The optimized Chemosensor **1** gave a flat structure with extended conjugation that allowed internal charge transfer (ICT); this may be the reason for the observed strong fluorescence at 405 nm (Figure 5). Upon addition of  $\text{H}_2\text{PO}_4^-$ , Chemosensor **1** generated a pseudocavity-like structure to accommodate  $\text{H}_2\text{PO}_4^-$  through intermolecular hydrogen bonding formed with the N,O-atoms of the Chemosensor **1**, as well as charge neutralization. Upon complexation, the flatness of the Chemosensor was disrupted, as well as ICT, which resulted in fluorescence quenching. The frontier molecular orbital plots of Chemosensor **1** and its  $\text{H}_2\text{PO}_4^-$  complex were further analyzed, indicating the highest occupied molecular orbital (HOMO) of **1** largely exists over  $-0.2324$  eV, whereas lowest unoccupied molecular orbital (LUMO) was over  $-0.1094$  eV (Figure 6). This ICT occurred within the Chemosensor **1**, but on complexation of **1** with  $\text{H}_2\text{PO}_4^-$ , the HOMO was distributed uniformly over the  $\text{H}_2\text{PO}_4^-$ , whereas the LUMO was found mainly around  $0.02729$  eV.

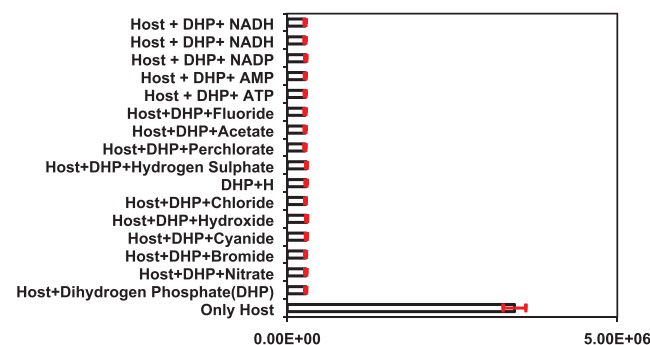


**FIGURE 4** Effect of competitive anions and biomolecules on  $\text{H}_2\text{PO}_4^-$  ion sensing

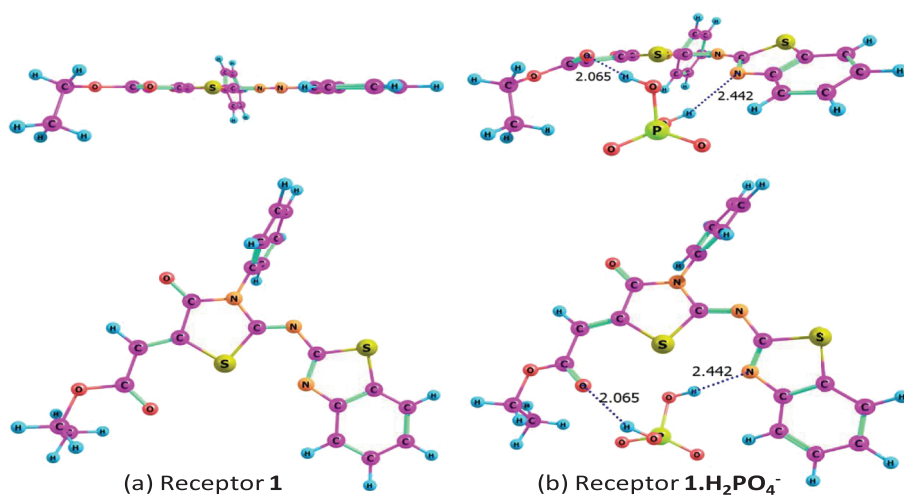


**FIGURE 5** Density functional theory DFT (B3LYP/6-311+G<sup>\*\*</sup>)-based optimized structure features of Chemosensor 1 (a) and its H<sub>2</sub>PO<sub>4</sub><sup>-</sup> complex (b) in the gas phase

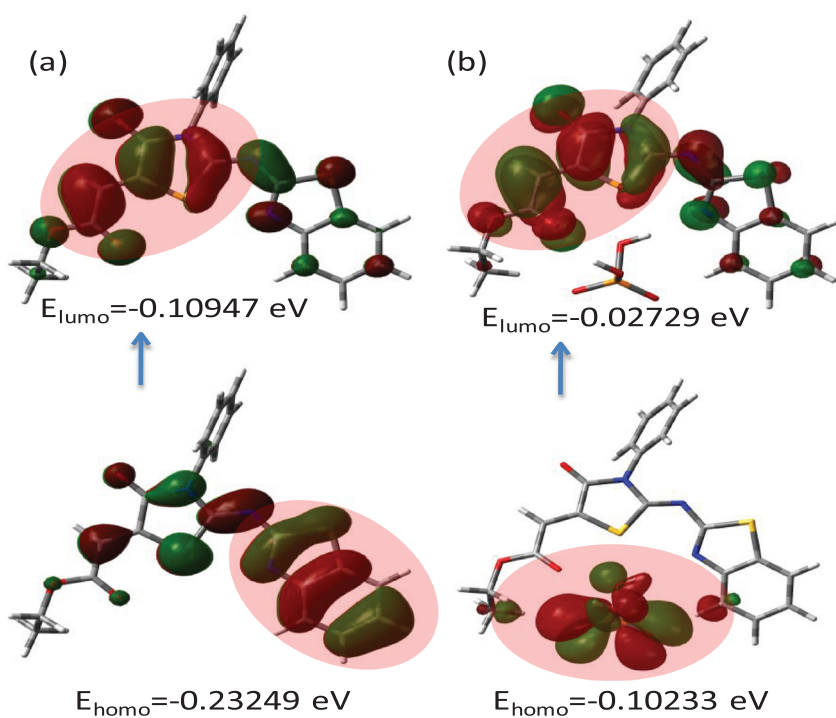


**FIGURE 6** Density functional theory (B3LYP/6-311+G<sup>\*\*</sup>)-based HOMO-LUMO positioning within the Chemosensor 1 (a) and its complex with H<sub>2</sub>PO<sub>4</sub><sup>-</sup> (b) in the gas phase

Therefore, charge transfer occurring within Chemosensor 1 is inhibited, and resulted in fluorescence quenching of Chemosensor 1.

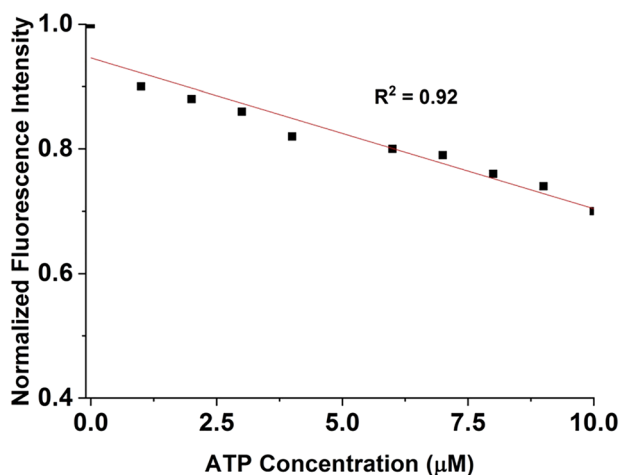
Furthermore, we proceeded with real sample analysis to tackle the effect of a matrix on sensing, albeit with the very few chemosensors available for the estimation of H<sub>2</sub>PO<sub>4</sub><sup>-</sup> ion in real sample analysis.<sup>[29]</sup> To examine the analytical application of Chemosensor 1, here we spiked different concentrations of tetrabutyl ammonium salt of H<sub>2</sub>PO<sub>4</sub><sup>-</sup> in tap water-, blood-, or urine-based samples. The developed sensor was then utilized to estimate the concentration of H<sub>2</sub>PO<sub>4</sub><sup>-</sup> in the prepared samples. The proposed sensor performed exceptionally well and concentration-dependent quenching in the fluorescence emission profile was observed with

no interference of the matrix. The estimated data, as well as actual concentrations of H<sub>2</sub>PO<sub>4</sub><sup>-</sup> in different samples, are summarized in Table 1.

Moreover, the sensor was also explored subsequently to investigate the activity profiling of apyrase enzyme. In this case, increasing concentrations of ATP along with apyrase were initially incubated overnight. The resulting solution so obtained was subsequently maintained at slightly acidic pH for 2 h. Finally, fluorescence profiling of the solutions was subsequently investigated using Chemosensor 1. Figure 7 revealed encouraging results, as continuous quenching was observed with increasing concentrations of ATP. Therefore, we have successfully utilized 1 to profile the ATPase activity of apyrase enzyme.

**TABLE 1** Real sample analysis of  $\text{H}_2\text{PO}_4^-$  in blood plasma, urine and tap water

Sample name	Actual concentration ( $\mu\text{M}$ )	Estimated concentration ( $\mu\text{M}$ )
Blood plasma	$10.24 \pm 0.03$	$10.33 \pm 0.01$
Tap water	$15.17 \pm 0.06$	$15.15 \pm 0.09$
Urine sample	$22.58 \pm 0.03$	$22.62 \pm 0.07$

**FIGURE 7** Fluorescence intensity versus concentration correlation graph (apyrase activity profiling with 1)

## 4 | CONCLUSION

A fluorogenic chemosensor containing competent response sites for the selective and sensitive detection of  $\text{H}_2\text{PO}_4^-$  ions at micromolar concentrations and in semiaqueous medium is reported. The sensing protocol proceeded via a standing emission quenching process based on inhibition of ICT through anion coordination. Computed density functional theory (DFT) results for anion recognition events were found to correlate with the experimental contour. DFT calculations indicated the formation of a noncovalent bonded (hydrogen bonded) aggregate between the imine and sulphur moiety of Chemosensor 1 and  $\text{H}_2\text{PO}_4^-$  anion, thereby endorsing quenching. The Chemosensor 1 was harmoniously opted for real sample analysis and for real-time monitoring of the concentrations of ATP in lysosomes with noteworthy results.

## ACKNOWLEDGEMENTS

The author YBW are grateful to Council of Scientific & Industrial Research (CSIR), New Delhi India for the postdoctoral research fellowship under CSIR-RA [Award No. 09/728(0036)/2019 (EMR-I)]. We are thankful to the University Grants Commission (UGC) New Delhi, India [F.4-6/2015/DSA-I (SAP-II)] for Financial assistance under the Special Assistance Programme (SAP) for infrastructural facilities.

## ORCID

Yogesh B. Wagh <https://orcid.org/0000-0002-3364-7519>Dipak S. Dalal <https://orcid.org/0000-0003-2934-0984>

## REFERENCES

- [1] H. Sharma, N. Kaur, A. Singh, A. Kuwar, N. Singh, J. Mater. Chem. C **2016**, 4, 5154.
- [2] [a] C. A. Huerta-Aguilar, T. Pandiyan, N. Singh, N. Jayanthi, Spectrochim. Acta A Mol. Biomol. Spectrosc. **2015**, 146, 142. [b] D. Huerta-Jose, J. G. Hernandez, C. A. Huerta-Aguilar, P. Thangarasu, Sens. Actuators B **2019**, 293, 357. [c] J. A. Ortega Granados, J. G. Hernandez, C. A. Huerta-Aguilar, P. Thangarasu, Sens. Actuators B **2018**, 270, 570.
- [3] [a] R. W. Catral, Chemical Sensors, Oxford University Press, Oxford **1997**. [b] J. G. Hernández, C. A. Huerta-Aguilar, P. Thangarasu, H. Hopflc, New J. Chem. **2017**, 41, 10815. [c] Y. S. García-Gutiérrez, C. A. Huerta-Aguilar, P. Thangarasu, J. M. Vazquez-Ramos, Sens. Actuators, B **2017**, 248, 447.
- [4] [a] J. P. Anzenbacher, P. Lubal, P. Bucek, M. A. Palacios, M. F. Kozelkova, Chem. Soc. Rev. **2010**, 39, 3954. [b] C. A. Huerta-Aguilar, T. Pandiyan, P. Raj, N. Singh, R. Zanella, Sens. Actuators B **2016**, 223, 59. [c] C. A. Huerta-Aguilar, P. Raj, P. Thangarasu, N. Singh, RSC Adv. **2016**, 6, 37944.
- [5] L. J. Fan, W. E. Jones, J. Am. Chem. Soc. **2006**, 128, 6784.
- [6] P. Worsfold, L. Gimbert, U. Mankasingh, O. Omaka, G. Hanrahan, P. Gardolinski, P. Haygarth, B. Turner, M. Keith-Roach, I. McKelvie, Talanta **2005**, 66, 273.
- [7] A. Bianchi, K. B. James, E. G. Espana, Supramolecular Chemistry of Anions, Wiley-VCH, New York, NY **1997**.
- [8] J. L. Sessler, P. A. Gale, W. S. Cho, Anion Chemosensor Chemistry, Monographs in Supramolecular Chemistry, Ed. J. F. Stoddart, RSC, Cambridge, UK **2006**.
- [9] R. Dutzler, E. B. Campbell, R. Mackinnon, Science **2003**, 300, 108.
- [10] M. Ronaghi, S. Karamohamed, B. Pettersson, M. Uhlen, P. Nyren, Anal. Biochem. **1996**, 242, 84.
- [11] S. Xu, M. He, H. Yu, X. Cai, X. Tan, B. Lu, B. Shu, Anal. Biochem. **2001**, 299, 188.
- [12] W. Saenger, Principles of Nucleic Acid Structure, New York, Springer **1988**.
- [13] H. Kawasaki, K. Sato, J. Ogawa, Y. Hasegawa, H. Yuki, Anal. Biochem. **1989**, 182, 366.
- [14] Q. Y. Cao, Z. C. Wang, M. Li, J. H. Liu, Tetrahedron Lett. **2013**, 54, 3933.
- [15] D. Zhang, X. Jiang, Z. Dong, H. Yang, A. Martinez, G. Gao, Tetrahedron **2013**, 69, 10457.
- [16] W. Gong, K. Hiratani, Tetrahedron Lett. **2008**, 49, 5655.
- [17] P. D. Beer, P. A. Gale, Angew. Chem. Int. Ed. **2001**, 40, 486.
- [18] A. K. Jain, A. Vaidya, V. Ravichandran, S. K. Kashaw, R. K. Agrawal, Bioorg. Med. Chem. **2012**, 20, 3378.
- [19] A. Verma, S. K. Saraf, Eur. J. Med. Chem. **2008**, 43, 897.
- [20] A. C. Tripathi, S. J. Gupta, G. N. Fatima, P. K. Sonar, A. Verma, S. K. Saraf, Eur. J. Med. Chem. **2014**, 72, 52.
- [21] (a) K. S. Dalal, Y. B. Wagh, Y. A. Tayade, D. S. Dalal, B. L. Chaudhari, Catal. Lett. **2018**, 148, 3335. (b) K. S. Dalal, S. A. Padvi, Y. B. Wagh, D. S. Dalal, B. L. Chaudhari, ChemistrySelect **2018**, 3, 10378.
- [22] (a) M. Kaur, P. Raj, N. Singh, A. Kuwar, N. Kaur, Eng. **2018**, 6, 3723. (b) P. Torawane, K. Keshav, M. K. Kumawat, R. Srivastava, T. Anand, S. Sahoo, A. Borse, A. Kuwar, Photochem. Photobiol. Sci. **2017**, 16, 1464.
- [23] Y. B. Wagh, A. S. Kuwar, D. R. Patil, Y. A. Tayade, A. D. Jangale, S. S. Terdale, D. R. Trivedi, J. Gallucci, D. S. Dalal, Ind. Eng. Chem. Res. **2015**, 54, 9675.
- [24] Y. B. Wagh, A. Kuwar, S. K. Sahoo, J. Gallucci, D. S. Dalal, RSC Adv. **2015**, 5, 45528.

- [25] W. T. Gong, D. Na, L. Fang, H. Mehdi, G. L. Ning, *Org. Biomol. Chem.* **2015**, *13*, 1979.
- [26] P. Job, *Ann. Chim.* **1928**, *9*, 113.
- [27] H. A. Benesi, J. H. Hildebrand, *J. Am. Chem. Soc.* **1949**, *71*, 2703.
- [28] M. J. Frisch, G. W. Trucks, H. B. Schlegel, G. E. Scuseria, M. A. Robb, J. R. Cheeseman, G. Scalmani, V. Barone, G. A. Petersson, H. Nakatsuji, X. Li, M. Caricato, A. Marenich, J. Bloino, B. G. Janesko, R. Gomperts, B. Mennucci, H. P. Hratchian, J. V. Ortiz, A. F. Izmaylov, J. L. Sonnenberg, D. Williams-Young, F. Ding, F. Lipparini, F. Egidi, J. Goings, B. Peng, A. Petrone, T. Henderson, D. Ranasinghe, V. G. Zakrzewski, J. Gao, N. Rega, G. Zheng, W. Liang, M. Hada, M. Ehara, K. Toyota, R. Fukuda, J. Hasegawa, M. Ishida, T. Nakajima, Y. Honda, O. Kitao, H. Nakai, T. Vreven, K. Throssell, J. A. Montgomery, Jr., J. E. Peralta, F. Ogliaro, M. Bearpark, J.J. Heyd, E. Brothers, K. N. Kudin, V. N. Staroverov, T. Keith, R. Kobayashi, J. Normand, K. Raghavachari, A. Rendell, J. C. Burant, S. S. Iyengar, J. Tomasi, M. Cossi, J. M. Millam, M. Klene, C. Adamo, R. Cammi, J. W. Ochterski, R. L. Martin, K. Morokuma, O. Farkas, J. B. Foresman, D. J. Fox, *Gaussian 09, Revision A.02*, Gaussian, Inc., Wallingford CT, **2016**.
- [29] S. Berchmans, T. B. Issa, P. Singh, *Anal. Chim. Acta* **2012**, *729*, 7.

#### SUPPORTING INFORMATION

Additional supporting information may be found online in the Supporting Information section at the end of this article.

**How to cite this article:** Wagh YB, Tayade KC, Kuwar A, et al. Exploration of highly selective fluorogenic 'on-off' chemosensor for  $\text{H}_2\text{PO}_4^-$  ions: ICT-based sensing and ATPase activity profiling. *Luminescence*. 2020;35:379–384. <https://doi.org/10.1002/bio.3737>